Cell Reports
Article

Addiction of t(8;21) and inv(16) Acute Myeloid Leukemia to Native RUNX1

Oren Ben-Ami,[1] Dan Friedman,[2] Dena Leshkowitz,[3] Dalia Goldenberg,[1] Kira Orlovsky,[1] Niv Pencovich,[1] Joseph Lotem,[1] Amos Tanay,[2] and Yoram Groner[1,*]
[1]Department of Molecular Genetics, Weizmann Institute of Science, 76100 Rehovot, Israel
[2]Department of Computer Science and Applied Mathematics, Weizmann Institute of Science, 76100 Rehovot, Israel
[3]Department of Biological Services, Weizmann Institute of Science, 76100 Rehovot, Israel
*Correspondence: yoram.groner@weizmann.ac.il
http://dx.doi.org/10.1016/j.celrep.2013.08.020

SUMMARY

The t(8;21) and inv(16) chromosomal aberrations generate the oncoproteins AML1-ETO (A-E) and CBFβ-SMMHC (C-S). The role of these oncoproteins in acute myeloid leukemia (AML) etiology has been well studied. Conversely, the function of native RUNX1 in promoting A-E- and C-S-mediated leukemias has remained elusive. We show that wild-type RUNX1 is required for the survival of t(8;21)-Kasumi-1 and inv(16)-ME-1 leukemic cells. RUNX1 knockdown in Kasumi-1 cells (Kasumi-1$^{RX1\text{-}KD}$) attenuates the cell-cycle mitotic checkpoint, leading to apoptosis, whereas knockdown of A-E in Kasumi-1$^{RX1\text{-}KD}$ rescues these cells. Mechanistically, a delicate RUNX1/A-E balance involving competition for common genomic sites that regulate RUNX1/A-E targets sustains the malignant cell phenotype. The broad medical significance of this leukemic cell addiction to native RUNX1 is underscored by clinical data showing that an active RUNX1 allele is usually preserved in both t(8;21) or inv(16) AML patients, whereas RUNX1 is frequently inactivated in other forms of leukemia. Thus, RUNX1 and its mitotic control targets are potential candidates for new therapeutic approaches.

INTRODUCTION

Acute myeloid leukemia (AML) is characterized by a block in early progenitor differentiation leading to accumulation of immature, highly proliferative leukemic stem cells (LSCs) in bone marrow (BM) and blood (Rosenbauer et al., 2005). Chromosome-21-encoded transcription factor (TF) RUNX1 (a.k.a. AML1) is a frequent target of various chromosomal translocations (Lam and Zhang, 2012). The most prevalent translocation in AML is t(8;21) (Hatlen et al., 2012; Müller et al., 2008), which creates a fused gene product designated AML1-ETO (A-E). It contains the DNA-binding domain of RUNX1 (the runt domain [RD]) linked to the major part of the chromosome-8-encoded protein ETO (Erickson et al., 1992; Miyoshi et al., 1993), which by itself lacks DNA-binding capacity (Davis et al., 2003).

RUNX1 is a key hematopoietic gene expression regulator in embryos and adults (Cameron and Neil, 2004; de Bruijn and Speck, 2004; Wang et al., 1996). Its major cofactor, core-binding factor β (CBFβ), is essential for RUNX1 function (Miller et al., 2001, 2002). On the other hand, ETO is a transcriptional repressor (Davis et al., 2003) that is known to interact with corepressors such as NCoR/SMRT, mSin3a, and histone deacetylases (HDACs) (reviewed in Hug and Lazar, 2004). Of note, although the *ETO* gene is normally expressed in the gut and CNS (Lam and Zhang, 2012), the t(8;21) translocation places it under transcriptional control of *RUNX1* regulatory elements (Bee et al., 2009; Ghozi et al., 1996; Levanon et al., 2001). This occurrence evokes expression of A-E in the myeloid cell lineage.

The prevailing notion is that A-E binds to RUNX1 target genes and acts as dominant-negative regulator, thereby producing conditions that resemble the RUNX1$^{-/-}$ phenotype (reviewed in Goyama and Mulloy, 2011; Hatlen et al., 2012; Lam and Zhang, 2012; Licht, 2001). Consistent with this concept, mice expressing an A-E knockin allele (Okuda et al., 1998; Yergeau et al., 1997) display early embryonic lethality and hematopoietic defects similar to those observed in Runx1$^{-/-}$ mice (reviewed in Goyama and Mulloy, 2011; Hatlen et al., 2012; Lam and Zhang, 2012; Licht, 2001). However, it has also been shown that A-E-mediated leukemogenicity involves other events that affect gene regulation, in addition to repression of RUNX1 targets (Bakshi et al., 2008; Hatlen et al., 2012; Hyde and Liu, 2010; Lam and Zhang, 2012; Okumura et al., 2008). Reduction of A-E expression in leukemic cells by siRNA restores myeloid differentiation (Dunne et al., 2006; Heidenreich et al., 2003; Martinez et al., 2004) and delays in vivo tumor formation (Martinez Soria et al., 2009). Depletion of A-E in t(8;21)$^{+}$ AML cells causes genome-wide changes in chromatin structure leading to redistribution of RUNX1 occupancy and inhibition of cell self-renewal capacity (Ptasinska et al., 2012).

An additional AML subtype associated with altered RUNX1 activity involves the chromosomal aberrations inv(16)(p13q22) and t(16;16)(p13q22) (abbreviated as inv(16)). This inversion

fuses the chromosome 16q22-encoded CBFβ gene with the MYH11 gene, which resides at 16p13 and encodes smooth-muscle myosin heavy chain (SMMHC). The resulting chimeric oncoprotein is known as CBFβ-SMMHC (Arthur and Bloomfield, 1983; Le Beau et al., 1983). Similarly to A-E, CBFβ-SMMHC (C-S) is a dominant inhibitor of RUNX1 activity (Castilla et al., 1996; Lukasik et al., 2002) that impairs myeloid differentiation and contributes to AML development (Castilla et al., 2004; Kuo et al., 2006).

Although the central role of A-E in the leukemic process has been extensively studied, the potential role of the wild-type (WT) RUNX1 allele in t(8;21) AML etiology remains unclear (Goyama and Mulloy, 2011). Similarly, the function of RUNX1 in the development of inv(16) AML is completely unknown. We used the AML cell lines t(8;21) Kasumi-1 (Asou et al., 1991) and inv(16) ME-1 (Yanagisawa et al., 1991) to evaluate the possible involvement of WT RUNX1 in A-E- and C-S-mediated leukemogenesis. We show that t(8;21) Kasumi-1 and inv(16) ME-1 AML cells are physiologically dependent on RUNX1 activity for their survival. The broad medical significance of this leukemic cell addiction to native RUNX1 is underscored by clinical data showing that an active *RUNX1* allele is maintained in both t(8;21) and inv(16) AML patients, whereas *RUNX1* is frequently inactivated in other forms of AML (Schnittger et al., 2011; Tang et al., 2009; reviewed in Goyama and Mulloy, 2011).

Knockdown (KD) of RUNX1 in Kasumi-1 cells (Kasumi-$1^{RX1\text{-}KD}$) results in A-E-mediated, caspase-dependent apoptosis. This apoptosis is triggered by the dysregulated expression of a gene subset that is crucial for mitotic functions, including mitotic checkpoint signaling. Significantly, KD of A-E in Kasumi-$1^{RX1\text{-}KD}$ cells evades this apoptosis and rescues Kasumi-$1^{RX1\text{-}KD}$, whereas KD of A-E diminishes the leukemogenic cell phenotype. Thus, a delicate balance between A-E and WT RUNX1 activities is required to maintain the malignant phenotype of Kasumi-1 cells. We elucidated the mechanism underlying this RUNX1/A-E balance by using combined differential gene expression and genome-wide chromatin immunoprecipitation sequencing (ChIP-seq) analyses. This analysis identified a subset of RUNX1/A-E common responsive genes that are inversely regulated by these two TFs and singled out the most critical RUNX1 targets. Our findings uncovered a previously unrecognized role of RUNX1 in the regulation of mitotic checkpoint events, through which it prevents the inherent apoptotic process in t(8;21) cells and facilitates leukemogenesis. These data implicate RUNX1 and its downstream mitotic regulators as potential targets for new therapeutic treatments of t(8;21) and inv(16) leukemias.

RESULTS

Expression of WT RUNX1 Is Essential for t(8;21) AML Kasumi-1 Cell Survival

We assessed the cell-phenotypic consequences of RUNX1 KD in Kasumi-1 cells to directly address the possibility that native RUNX1 function is required for the leukemogenic process in t(8;21) AML cells. Specific siRNA-oligo nucleotides that target *RUNX1* regions absent from the A-E transcript were used to attenuate the expression of RUNX1 (Figures 1A and S1A). Cell-cycle analysis of Kasumi-$1^{RX1\text{-}KD}$ cells revealed a prominent increase in the proportion of cells bearing subG1 DNA content and a significant decrease in the proportions of S and G2/M phases as compared with cells transfected with control nontargeting (NT) siRNA (Kasumi-1^{Cont}; Figures 1B, 1C, S1B, and S1C). This abnormal Kasumi-$1^{RX1\text{-}KD}$ cell cycle was associated with an elevated percentage of both Annexin-V^+ viable and nonviable cells (Figure 1D) and a ~7-fold decrease in the total number of viable cells (Figure 1E). These results indicated that KD of RUNX1 induces apoptotic cell death in Kasumi-$1^{RX1\text{-}KD}$. Transfection of an alternative siRNA oligo directed against a different *RUNX1* region (indicated by the orange bar in Figure 1A) confirmed that apoptosis resulted from decreased RUNX1 activity (Figure S2) and ruled out the possibility of a siRNA-specific off-target effect.

We next sought to determine whether Kasumi-$1^{RX1\text{-}KD}$ cell death involves the mitochondrial permeability transition (MPT). Flow-cytometry imaging (ImageStream System) analysis demonstrated that increased Kasumi-$1^{RX1\text{-}KD}$ cell apoptosis was associated with loss of mitochondrial membrane potential (Figures 1F and 1G), suggesting the involvement of MPT in inducing cell death. To assess whether this RUNX1 KD-triggered apoptosis involved caspase activation, we analyzed Kasumi-$1^{RX1\text{-}KD}$ and Kasumi-1^{Cont} cell cycles in the presence of the broad-spectrum caspase inhibitor *Z-VAD-FMK*. Significantly, *Z-VAD-FMK* completely blocked apoptosis in Kasumi-$1^{RX1\text{-}KD}$ cells, as reflected in a profound decrease of the subG1 fraction to a level similar to that of Kasumi-1^{Cont} cells (Figure 1H). Of note, the majority of *Z-VAD-FMK*-rescued Kasumi-$1^{RX1\text{-}KD}$ cells accumulated at cell-cycle G1 and G2/M phases (Figure 1H), suggesting that RUNX1 KD-evoked apoptosis involved impaired G2/M-to-G1 and G1-to-S transitions. Using *Z-VAD-FMK*-treated cells, we also recorded reduced RUNX1 protein levels in Kasumi-$1^{RX1\text{-}KD}$ cells (Figure 1I). Taken together, the results of the cell-cycle analysis, Annexin-V staining, viability assay, ImageStream analysis, and *Z-VAD-FMK* experiments demonstrate that attenuation of WT RUNX1 expression in Kasumi-1 cells triggers pronounced caspase-dependent apoptosis associated with changes in mitochondrial permeability. The most likely implication of these data is that WT RUNX1 plays an antiapoptotic role in t(8;21) AML cells and its activity is compromised by the oncogenic A-E bearing the RUNX RD. Therefore, the remaining WT RUNX1 activity is indispensable for cell viability.

A-E KD Rescues Kasumi-$1^{RX1\text{-}KD}$ Cells from Apoptosis

To further investigate the involvement of WT RUNX1 in the development of A-E-mediated t(8;21) AML, we used siRNA specific for the translocated transcripts to KD A-E (Kasumi-$1^{AE\text{-}KD}$) expression (Figures 2A and S3A, top). Kasumi-$1^{AE\text{-}KD}$ cells displayed decreased proliferation (Figure S3A, bottom) and increased myeloid differentiation (Figures S3B and S3C), as was previously noted (Dunne et al., 2006; Heidenreich et al., 2003; Martinez et al., 2004; Ptasinska et al., 2012), as well as a marked reduction in the proportion of $CD34^+CD38^-$ leukemogenic cell population (Figures S3B and S3C). We next examined the impact of A-E KD on the cell phenotype of Kasumi-$1^{RX1\text{-}KD}$. Interestingly, the double-KD cells (Kasumi-$1^{RX1/AE\text{-}KD}$) displayed an apoptotic level similar to or even lower than that of control cells (Figures

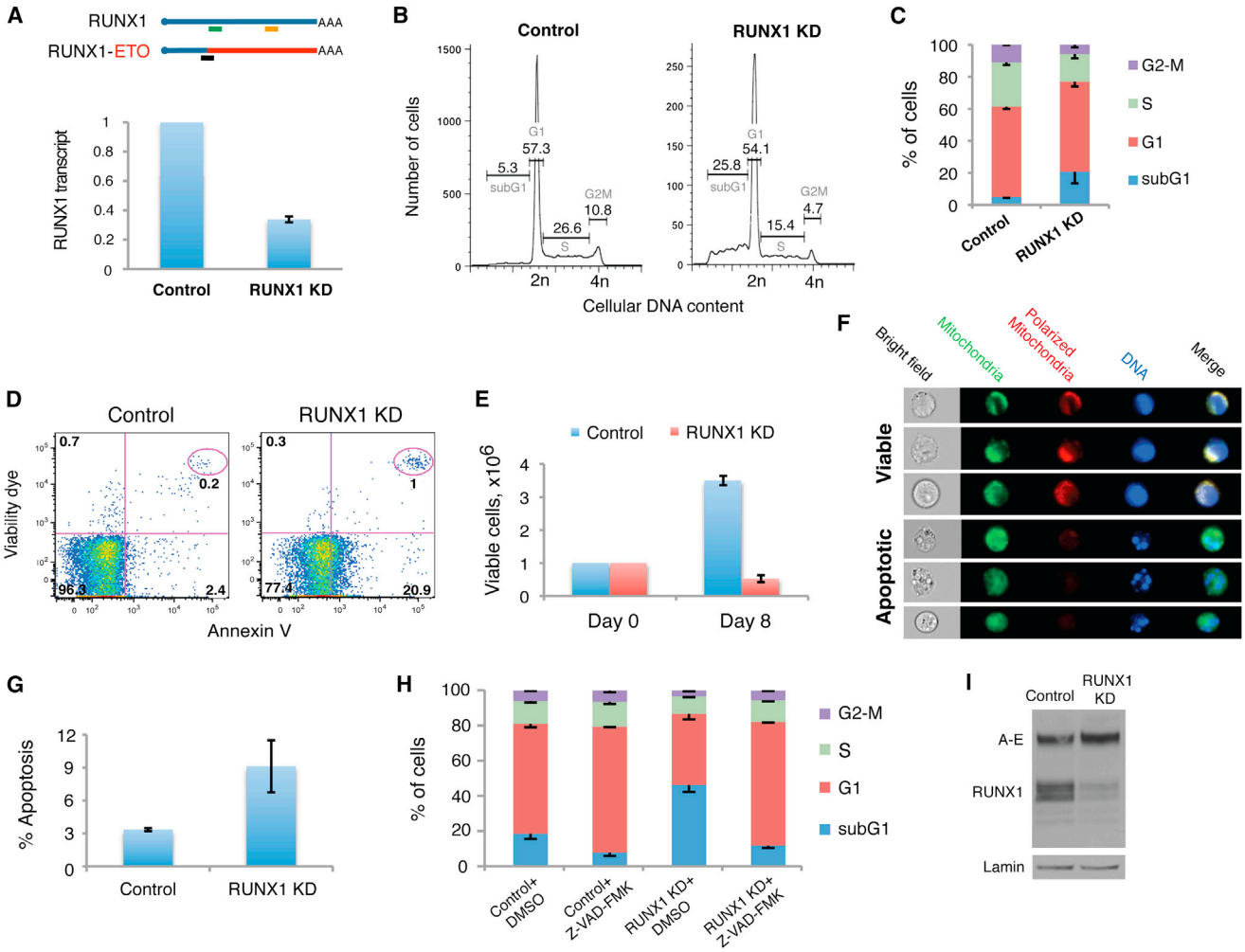

Figure 1. WT RUNX1 Prevents Apoptosis of the t(8;21) Kasumi-1 Leukemic Cell Line

(A) Upper panel: scheme of RUNX1 (blue) and RUNX1-ETO (A-E, blue-red) transcripts indicating regions targeted by the siRNAs used to knock down expression of either *RUNX1* (bars underneath RUNX1 marked in green and orange) or *A-E* (black bar underneath the A-E fusion region). Lower panel: qRT-PCR analysis of siRNA-mediated *RUNX1* KD. Total RNA was isolated 24 hr after electroporation of RUNX1-targeting or NT control siRNA. The data shown represent mean expression ± SE. Shown are results from one of three experiments with the same findings. Primers used for qRT-PCR are presented in Table S7.

(B and C) Cell-cycle analysis 8 days posttransfection with either RUNX-targeting or NT siRNA.

(B) Cells were subjected to two successive transfections (at days 0 and 4) with either RUNX1-targeting or NT siRNA. Propidium iodide (PI) was used to assess cellular DNA content by FACS analysis. Bar numbers indicate the relative size (in %) of the labeled population out of total cells. Indicated cell-cycle phases: subG1, G1, S, and G2M (see also Figure S1).

(C) Histograms summarizing the distribution of cell population as analyzed in (B). Data represent the mean ± SD values of five independent experiments.

(D) Increased Kasumi-1$^{RX1\text{-}KD}$ cell apoptosis. Cells were stained with Annexin-V following siRNA-mediated RUNX1 KD. Staining with the eFluor780 viability dye marked dead/late apoptotic cells. Results from one of two experiments with the same findings are shown. See also Figure S2.

(E) Diminished Kasumi-1$^{RX1\text{-}KD}$ cell viability. Eight days posttransfection with either RUNX1-targeting or NT siRNA, the total number of viable cells was assessed via standard hemocytometer cell counting excluding trypan-blue-stained cells. Data represent the mean ± SD values of three independent experiments.

(F and G) RUNX1 KD-induced apoptosis is associated with loss of mitochondrial membrane potential.

(F) ImageStream System analysis of Kasumi-1 cells incubated for 4 days with RUNX1-targeting or NT siRNA and stained for cell mitochondria and DNA content. Bright-field visualization indicates cell apoptotic morphology. Green fluorescent dye (Mitogreen) stains mitochondria in both live and dead cells. Red dye (MitoTracker Red CMXRos) stains mitochondria only in live cells, depends on mitochondrial membrane potential, and indicates MPT. DNA was stained with DRAQ5. Cells with a low red/green ratio and low DNA signal were defined as apoptotic. Results from one of two experiments with the same findings are shown.

(G) Histograms presenting quantitative data of ImageStream System analysis for Kasumi-1$^{RX1\text{-}KD}$ and Kasumi-1^{Cont} as mean ± SD of two biological repeats.

(H) Caspase inhibition rescues Kasumi-1$^{RX1\text{-}KD}$ from apoptosis. Three days after siRNA delivery, cells were incubated with either Z-VAD-FMK (50 μM) or vehicle (DMSO) for an additional 24 hr. Histograms show the distribution of cells among cell-cycle phases determined as detailed above. The data shown represent the mean ± SD of four independent experiments.

(I) Western blot analysis demonstrating RUNX1 KD. Cells transfected with RUNX1-targeting or NT siRNA were incubated for 72 hr followed by additional 24 hr incubation with Z-VAD-FMK (50 μM). Blots were reacted with Ab against RUNX1-N terminus or Lamin. Results from one of two experiments with the same findings are shown. See also Figure S1A.

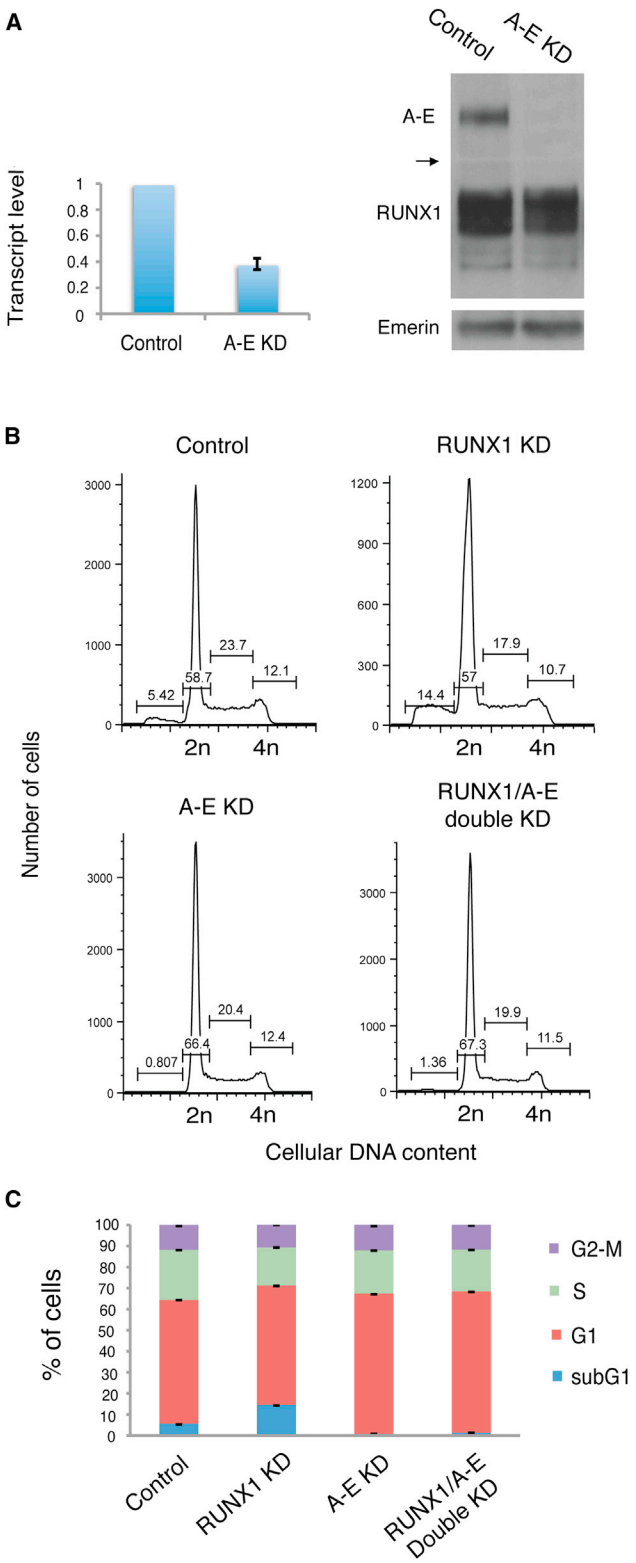

Figure 2. Rescue of Kasumi-1$^{RX1\text{-}KD}$ Cells from Apoptosis by KD of A-E

(A) Specific reduction of A-E expression in Kasumi-1$^{AE\text{-}KD}$ cells. Expression of A-E and RUNX1 following cell transfection with A-E- or RUNX1- targeting (indicated in Figure 1A by black and green bars, respectively) or control siRNAs was analyzed by qRT-PCR (left panel) 24 hr posttransfection, and by western blotting (right panel) using anti ETO, anti RUNX1, or anti lamin Abs 96 hr posttransfection. To rigorously monitor the specificity of A-E KD, the blot was divided as indicated by the black arrow, and the upper and lower parts were reacted with anti-ETO or anti-RUNX1 C-terminal Abs, respectively (Extended Experimental Procedures).

(B and C) KD of A-E rescues Kasumi-1 cells from RUNX1 KD-induced apoptosis. Cells were cotransfected with a 1:1 mixture of RUNX1 and A-E targeting siRNAs or separately with RUNX1 siRNA, A-E siRNA, or NT siRNA.

(B) Following incubation for 8 days, cells were stained with PI and analyzed by FACS for cell cycle.

(C) Histograms show the distribution of cells among cell-cycle phases. Data shown represent the mean ± SD of four independent biological repeats.

See also Figure S3.

2B and 2C). This observation is consistent with the possibility that A-E activity contributed to Kasumi-1$^{RX1\text{-}KD}$ cell apoptosis, underscoring the importance of the balance between A-E and RUNX1 activities for maintaining leukemogenicity. It further suggests that A-E and RUNX1 serve as positive and negative apoptosis regulators, respectively, by controlling the expression of their shared target genes in an opposing manner.

RUNX1- and A-E-Responsive Genes Are Inversely Regulated

We next sought to identify RUNX1- and A-E-responsive genes that participate in the interplay between the two TFs, thereby affecting Kasumi-1 cell survival. First, we assessed the global gene expression alterations in response to KD of either RUNX1 or A-E by analyzing the Kasumi-1$^{RX1\text{-}KD}$ or Kasumi-1$^{AE\text{-}KD}$ cell transcriptomes compared with that of Kasumi-1^{Cont} (Tables S1 and S2). Importantly, the overall gene expression profile in response to KD of A-E or RUNX1 was inversely correlated (Figure 3A, $R^2 = -0.33$). Genes that were repressed following RUNX1 KD tended to be upregulated following A-E KD and vice versa (Figure 3A).

Of the 754 genes that responded to KD of either A-E or RUNX1, 109 were common and affected by KD of either one (Figure 3B). The majority of these A-E/RUNX1 common genes (95 of 109) responded inversely to the KD of RUNX1 or A-E (Table S3). Interestingly, analysis of these inversely A-E/RUNX1-regulated genes (using Ingenuity System IPA) revealed a significant association with terms of cell death and/or apoptosis (Table S4). Thus, the gene expression data supported the idea that disruption of the cellular balance between RUNX1 and A-E activities is the underlying cause of Kasumi-1$^{RX1\text{-}KD}$ cell apoptosis. We therefore further characterized this regulatory interplay by analyzing the genomic occupancy of the two TFs.

RUNX1 and A-E Genomic Occupancy Patterns

To selectively map the genomic occupancy of either RUNX1 or A-E, we conducted ChIP-seq using anti-RUNX1-C terminus or anti-ETO specific antibodies (Figure 3C). Data analysis revealed 14,247 RUNX1-bound genomic regions and a comparable number of A-E bound regions (13,070). As could have been predicted from their common DNA-binding RD, the genomic occupancy of RUNX1 and A-E was highly correlated (Figures 3D and 3E). Despite this strong quantitative correlation, we also noted a

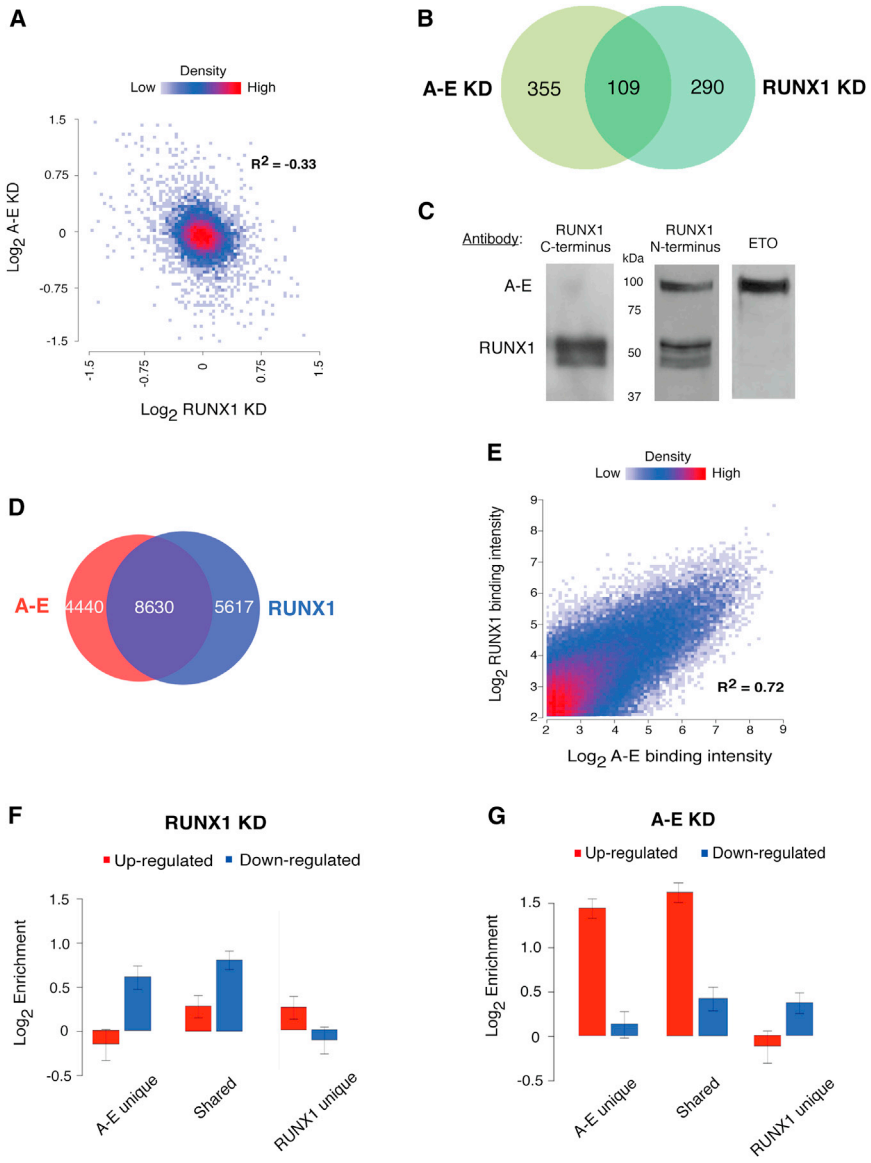

Figure 3. Gene Expression and ChIP-Seq Analysis of A-E- and RUNX1-Occupied Genomic Regions

(A) Gene expression profiling of Kasumi-1 following KD of either RUNX1 or A-E revealed a significant inverse gene expression response as evidenced by a negative Spearman correlation ($R^2 = -0.33$).

(B) Venn diagram showing the number and relative proportion of genes whose expression significantly changed following KD of either RUNX1 or A-E. The differential expression cutoff was set to a minimal absolute fold change of 1.4 and maximal p value of 0.05. See also Tables S1, S2, S3, and S4.

(C) Selective detection of RUNX1 or A-E proteins in Kasumi-1 cells. Western blotting of Kasumi-1 nuclear extracts using antibodies raised against the RUNX1-C terminus (left lane) or against ETO (right lane). The central lane was reacted with anti-RUNX1-N terminus antibody detecting both RUNX1 and A-E.

(D) Venn diagram of the number and relative proportion of RUNX1- and/or A-E-occupied genomic regions recorded by ChIP-seq experiments using anti-RUNX1-C terminus or anti-ETO.

(E) Comparison of RUNX1 and/or A-E binding affinity detected by ChIP-seq analysis. Binding of A-E and RUNX1 strongly correlated (Pearson $R^2 = 0.72$, p value $< 2 \times 10^{-16}$).

(F and G) Enrichment of genes up- and down-regulated in response to KD of RUNX1 (F) and A-E (G), respectively. Data were compiled using integrated results of ChIP-seq and gene expression. Shown are enrichment ratios for up- and down-regulated genes computed as the fraction of bound regulated genes divided by the global fraction of bound genes. Bars mark binomial SDs for the enrichment estimates.

See also Figure S3.

spectrum of differential A-E/RUNX1 binding (Figures 3E and S3D–S3G), suggesting variable binding affinities of the two TFs at loci with different genomic contexts.

To study the impact of binding patterns on the transcriptional response to KD of either RUNX1 or A-E, we integrated the ChIP-seq and gene expression data sets. A significant number of genes proximal to RUNX1/A-E-shared regions were downregulated following RUNX1 KD and upregulated in response to A-E KD (Figures 3F and 3G), supporting the notion that direct competition between the two TFs is the underlying mechanism driving the leukemogenic transcriptional program. Specifically, due to their common DNA-binding domain, RUNX1 and A-E occupy a shared subset of target genes. Because these genes are oppositely regulated by the two TFs, the cellular phenotypes of RUNX1 and A-E KD differ. However, the opposing regulatory effect of A-E and RUNX1 was also manifested in inverse regulation of their uniquely occupied genes (Figures 3F and 3G). This observation suggests that the two TFs might also compete indirectly due to distinct sequence affinities and/or interaction with cooperating TFs.

Comparative Sequence Analysis of Uniquely Occupied RUNX1/A-E Genomic Regions

The opposing transcriptional responses of RUNX1 and A-E shared and unique target genes prompted us to further characterize the properties of A-E- and/or RUNX1-bound regions. In comparison with uniquely A-E-bound regions, a significantly higher proportion of RUNX1-unique peaks were localized at the vicinity of the transcription start site (TSS; Figure 4A), suggesting that RUNX1 has an advantage over A-E in binding to promoter regions in Kasumi-1 cells. Sequence analysis of genomic regions uniquely bound by either A-E or RUNX1 revealed a significantly lower frequency of the canonical RUNX motif within A-E-bound regions (Figure 4B, left). On the other

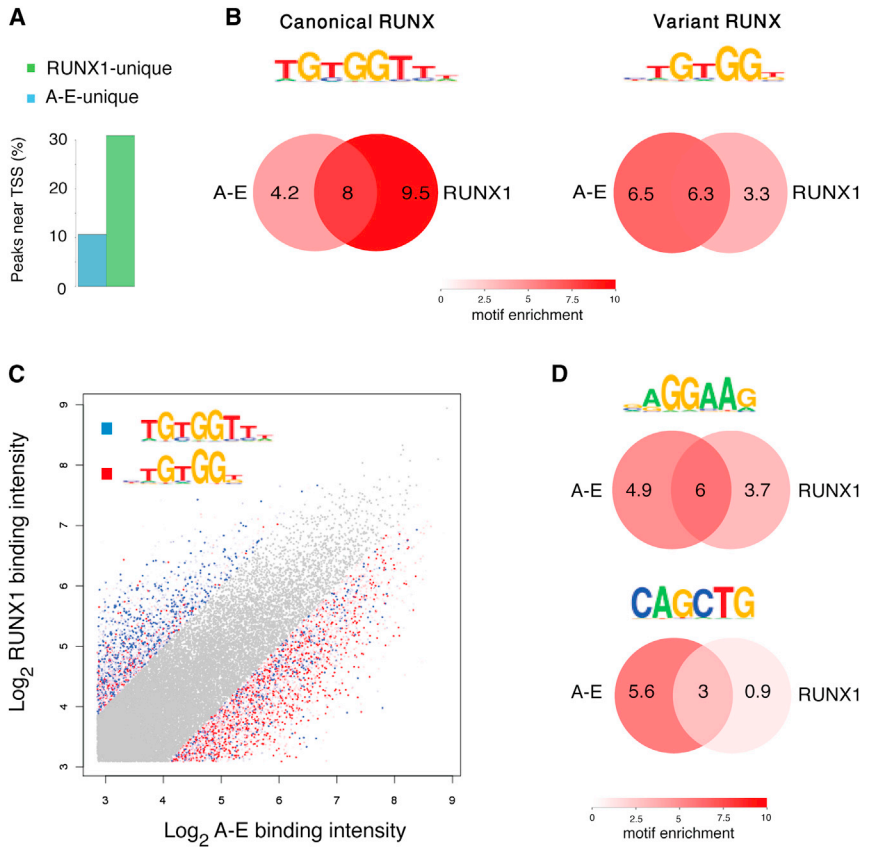

Figure 4. Comparative Sequence Analysis of RUNX1- and A-E-Bound Regions

(A) Frequency of uniquely bound RUNX1 or A-E proximal to annotated TSS. Bound TF was defined as proximal when the distance to annotated TSS was <500 bp.

(B) Enrichment of the canonical RUNX motif (left) and a RUNX-variant motif (right) in regions uniquely bound by RUNX1 or A-E. The level of motif enrichment is coded numerically (0 = no enrichment, 10 = high enrichment) and by color intensity in the Venn diagrams.

(C) The ratio of ChIP-seq binding intensities of RUNX1 and A-E is positively correlated with the relative enrichment of the canonical and variant RUNX motifs. Shown are binding intensities color-coded according to motif enrichments ratios: blue, high enrichment of canonical RUNX motif (observed mostly at upper left); red, high enrichment of variant RUNX motif (observed mostly at lower right).

(D) Enrichment of the ETS (upper) and AP4 (lower) TF motifs among unique and common RUNX1/A-E bound regions. Motifs were identified de novo using A-E and RUNX1 ChIP-seq genomic bound regions. The level of enrichment is indicated both numerically and by color as in (B). See also Figure S4.

hand, these A-E-occupied regions exhibited a higher frequency of a variant RUNX motif compared with the uniquely bound RUNX1 peaks (Figure 4B, right). Interestingly, the ratio between the two motifs quantitatively predicted the ratio between RUNX1 and A-E ChIP-seq enrichment (Figure 4C, $p < 2.2 \times 10^{-16}$). The enrichment of promoter occupancy by RUNX1 and the differential affinities of A-E and RUNX1 to the variant and canonical RUNX motifs suggest that subtle sequence preferences contributed to the differential binding and consequent biological activity of the two TFs.

Further sequence analysis of RUNX1- and A-E-occupied regions revealed that while both bound regions were enriched for the ETS TF motif (Figure 4D, top), only A-E unique regions were specifically enriched for the palindromic motif CAGCTG, bound by the E box TF AP4 (Figure 4D, bottom). The latter observation is consistent with previous studies (Gardini et al., 2008; Zhang et al., 2004) indicating that A-E interactions with E box proteins facilitate its binding to the DNA, and with the more recent finding of enrichment in E-Box-binding proteins among A-E-unique peaks (Ptasinska et al., 2012). Given that AP4 is highly expressed in Kasumi-1 cells (Figure S4A), we performed AP4 ChIP-seq and compared the distribution of AP4-binding sites with the A-E and RUNX1 occupancy profiles. Although significant numbers of ChIP-seq peaks were common to the three TFs, there was no preference for A-E/AP4 co-occupancy compared with that of RUNX1/AP4 (Figure S4B). This finding would argue that AP4 is unlikely to be the only E box TF that preferentially interacts with A-E. Nevertheless, we cannot rule out the possibility that A-E and AP4 regulate a common subset of genes in Kasumi-1 cells, potentially through protein-protein interaction as recently reported for AP4 and RUNX1 (Egawa and Littman, 2011). The ChIP-seq analysis may explain the mechanism underlying the opposing regulatory effects of RUNX1 and A-E, suggesting that sequence context and protein-protein interactions play a role in their overall impact on the cell-transcriptional program.

Gene Expression Analysis of Apoptosis-Inhibited Kasumi-$1^{RX1\text{-}KD}$ Cells Revealed Altered Expression of Critical Mitotic Progression Genes

Because RUNX1 KD in Kasumi-1 cells triggered extensive caspase-dependent apoptosis (Figure 1), we sought to identify the molecular pathways involved in this process. We measured differential gene expression in Z-VAD-FMK-treated Kasumi-$1^{RX1\text{-}KD}$ cells (Kasumi-$1^{RX1\text{-}KD+Z}$) compared with Z-VAD-FMK-treated control cells (Kasumi-1^{Cont+Z}; see Figures 1H and 1I).

Gene expression analysis revealed that 920 genes were differentially expressed in Kasumi-$1^{RX1\text{-}KD+Z}$ compared with Kasumi-1^{Cont+Z} cells (Figure 5A; Table S5). Out of these RUNX1-responsive genes, 485 and 435 genes were up- or down-regulated, respectively. Functional annotation analysis indicated that Kasumi-$1^{RUNX1\text{-}KD+Z}$ differentially expressed genes were highly enriched for genes with critical functions in mitosis (Table S6). This unique RUNX1-responsive mitotic subset included genes involved in regulation of the mitotic checkpoint, also known as the spindle-assembly checkpoint (SAC) (Lara-Gonzalez et al., 2012). Expression of several key mitotic

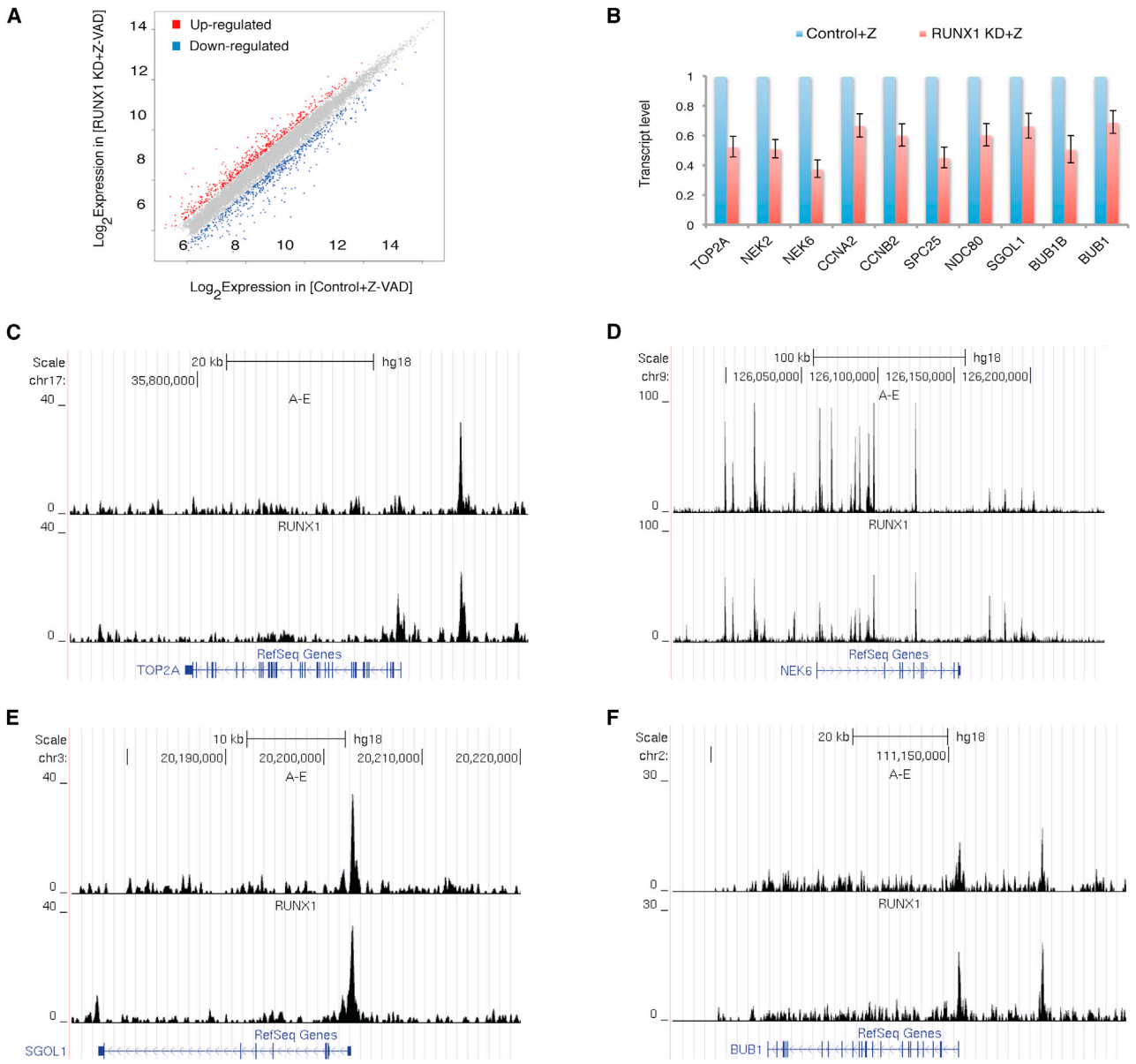

Figure 5. Transcriptome Analysis of Z-VAD-FMK-Treated Kasumi-1$^{RX1\text{-}KD}$ Cells Highlights a Gene Subset that Is Crucial for Mitotic Function

(A) Gene expression profile of Z-VAD-FMK-treated Kasumi-1$^{RX1\text{-}KD}$ cells. A scatterplot of differentially expressed genes in Kasumi-1 cells treated with control NT or RUNX1-targeting siRNA for 96 hr is shown. Z-VAD-FMK (50 μM) was added for the last 36 hr prior to FACS sorting of FITC$^+$ cells for RNA isolation. Genes that were up- or down-regulated due to RUNX1 KD are marked by red or blue dots, respectively. The differential expression cutoff was set to a minimal absolute fold change of 1.4 and maximal p value of 0.05. See also Tables S5 and S6.

(B) qRT-PCR analysis of mitotic genes scored by microarray gene expression. Results are presented as mean ± SE of two biological repeats.

(C–F) RUNX1 and A-E exhibit a similar binding pattern in *TOP2A*, *NEK6*, *SGOL1*, and *BUB1* genomic loci. Shown are ChIP-seq tracing wiggle files uploaded to the UCSC Genome Browser hg18 genome assembly.

and SAC genes that were downregulated in Kasumi-1$^{RX1\text{-}KD+Z}$ was validated by quantitative RT-PCR (qRT-PCR; Figure 5B). Interestingly, among these responsive genes, the genomic loci of *TOP2A*, *NEK6*, *SGOL1*, and *BUB1* exhibited similar ChIP-seq occupancy of RUNX1 and A-E (Figures 5C–5F). Additionally, Kasumi-1$^{RX1\text{-}KD+Z}$ expression data were also enriched for decreased expression of genes that are critical for DNA replication, including *PRIM1*, *ORC1L*, *RFC1*, *CDC6*, *MCM6*, and *MCM10* (Table S5). Taken together, these results suggest that in addition to its requirement in mitosis, RUNX1 might be critical for the proliferation of Kasumi-1 through its function in G1 and/or S phases. Collectively, these data are compatible with the possibility that RUNX1 positively regulates these mitosis-critical genes, but its KD in Kasumi-1$^{RX1\text{-}KD}$ cells enables A-E to bind

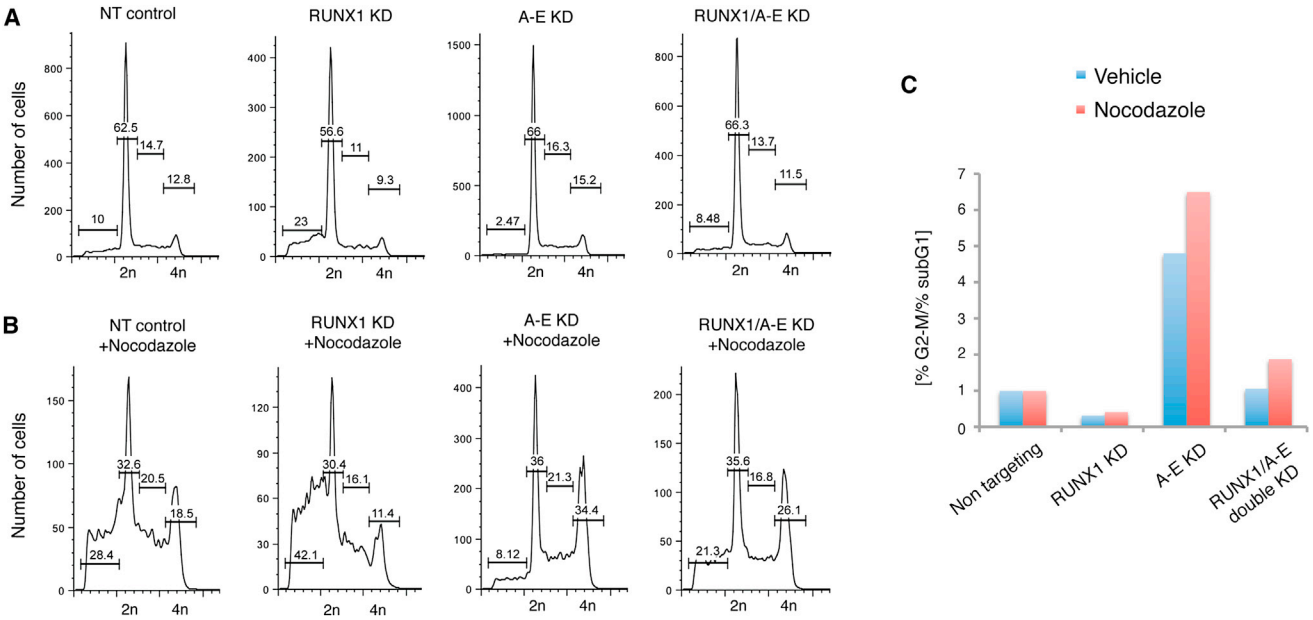

Figure 6. Opposing Effects of A-E and RUNX1 on SAC Signaling in Kasumi-1 Cells

(A and B) SAC signaling is regulated by RUNX1 and A-E. Cells were transfected with the indicated siRNAs and incubated for 72 hr prior to addition of (A) vehicle (DMSO) or (B) NOC (0.1 μg/ml) for 14 hr thereafter. Cell-cycle analysis was performed by FACS using PI labeling as described in Figure 1B. Bar numbers indicate the relative population size (in %) out of total cell number. Results from one of three experiments with similar findings are shown.

(C) The relative activity of RUNX1 and A-E impact SAC efficacy and thus a cell's tendency to undergo apoptosis. Histogram shows the ratio of % cells in G2/M versus subG1. The ratio calculated for the NT group was considered as one.

and repress their expression, resulting in mitotic impairment-mediated apoptosis.

Opposing Effects of RUNX1 and A-E on SAC Signaling

As a sensitive measurement of SAC activity, we used the microtubule-depolarizing agent nocodazole (NOC), which induces SAC, causing cell arrest at M phase. We asked how the induced changes in RUNX1 and A-E levels affect SAC signaling. Accordingly, we characterized the cell cycle of NOC-treated Kasumi-1^{Cont}, Kasumi-1$^{RX1\text{-}KD}$, Kasumi-1$^{A\text{-}E\text{-}KD}$, and double-KD Kasumi-1$^{RX1/A\text{-}E\text{-}KD}$ cells compared with cells treated with vehicle (Figures 6A and 6B).

Overall, the ability of NOC-treated cells to arrest cell cycle at M phase was inversely correlated with the proportion of dead/apoptotic cells that accumulated in subG1 (Figure 6B). Specifically, NOC-treated Kasumi-1$^{RX1\text{-}KD}$ and Kasumi-1$^{A\text{-}E\text{-}KD}$ cells displayed a diminished or elevated capacity, respectively, to arrest at M phase compared with NOC-treated Kasumi-1^{Cont} cells. Consequently, the proportion of their subG1 populations was increased (Kasumi-1$^{RX1\text{-}KD}$) or decreased (Kasumi-1$^{A\text{-}E\text{-}KD}$) (Figure 6B). Of particular relevance to this finding is the observation that cells expressing a C-terminal truncated isoform of A-E, designated A-Etr, display enhanced mitotic progression upon NOC treatment (Boyapati et al., 2007).

The complementary outcomes of these experiments suggest that whereas RUNX1 positively regulates SAC activity, A-E represses it. The findings that KD of A-E in Kasumi-1$^{RX1\text{-}KD}$ cells (Kasumi-1$^{RX1/AE\text{-}KD}$) restored SAC activity (Figure 6B) and rescued cells from apoptosis (Figures 2B and 2C) support this conclusion. Significantly, the opposing regulatory effects of A-E and RUNX1 on cellular gene expression noted above are reflected here in their impact on the cell ability to arrest at M phase and avoid cell death (Figure 6C). Thus, a threshold of WT RUNX1 activity is essential in t(8;21) AML cells to counter A-E-mediated inhibition of SAC signaling and thereby prevent complete disruption of SAC and subsequent apoptosis, possibly due to mitotic catastrophe.

Reduced RUNX1 Activity Affects inv(16) ME-1 and Preleukemic CD34$^+$/A-E Cell Viability

We next addressed whether the addiction of t(8;21) Kasumi-1 cell line to RUNX1 constitutes a common phenomenon in leukemia associated with partial loss of RUNX1 function. Using the inv(16) AML cell line ME-1 (Yanagisawa et al., 1991), we examined the impact of RUNX1 KD on cell survival. Significantly, RUNX1 KD (Figure 7A) produced a marked increase in Annexin-V staining of both viable and nonviable cells (Figure 7B), indicating RUNX1 KD-mediated enhancement of apoptosis.

Cell-cycle analysis of untreated ME-1 cells identified a mixed population of diploid and tetraploid cells (Figure S5), which is characteristic of cells with attenuated mitotic functions. This abnormal ME-1 cell-cycle profile made it unfeasible to record cell death based on DNA content analysis. The data suggest that the viability of inv(16) ME-1 cells, similarly to that of t(8;21) Kasumi-1 cells, physiologically depends on RUNX1 activity. The observations that inv(16) AML patients have no inactivating mutations in *RUNX1* (Döhner and Döhner, 2008; Goyama and

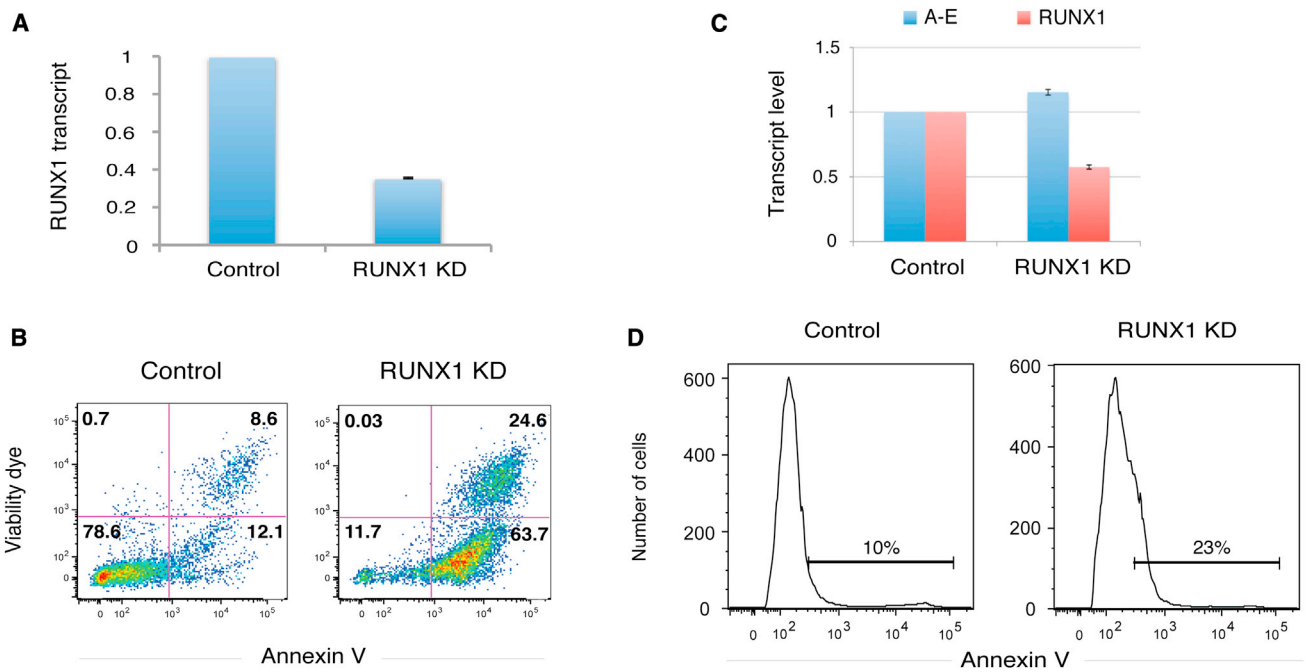

Figure 7. Requirement of Native RUNX1 for inv(16) ME-1 and Preleukemic CD34$^+$/A-E Cell Viability

(A and B) RUNX1 activity is essential for survival of the inv(16) ME-1 cell line.

(A) qRT-PCR demonstrating RUNX1 KD in ME-1 cells. RNA from cells 24 hr posttransfection with RUNX1-targeting or NT siRNA was analyzed by qRT-PCR. Results are the mean expression ± SE values of two experiments with similar results.

(B) KD of RUNX1 enhances apoptosis of ME-1 cell line. Cells were subjected to two successive rounds of electroporation (days 0 and 5) with either RUNX1-targeting or NT siRNA. On day 10, apoptosis was monitored by FACS analysis of Annexin-V-stained cells. Results from one of four experiments with similar findings are shown. See also Figure S5.

(C) qRT-PCR demonstrating RUNX1 KD in CD34$^+$/A-E cells. RNA from CD34$^+$/A-E cells 24 hr posttransfection with RUNX1-targeting or NT siRNA was analyzed by qRT-PCR. Results are the mean expression ± SE values of two experiments with similar results.

(D) KD of RUNX1 increased apoptosis of CD34$^+$/A-E cells. Twelve days after transduction with A-E lentiviral vector, cells were transfected with either RUNX1-targeting or NT siRNA, and 4 days later GFP$^+$ cells were assayed for Annexin-V staining by FACS. Histograms demonstrate a 2-fold increase in the proportion of Annexin-V-positive CD34$^+$/A-E cells among RUNX1 KD in comparison to control cultures. Results from one of three experiments with similar findings are shown.

Mulloy, 2011; Schnittger et al., 2011; Tang et al., 2009) or *CBFβ* (Heilman et al., 2006) further support this conclusion.

To evaluate the involvement of WT RUNX1 in the development of A-E-mediated preleukemic cell phenotype, we used a preleukemic cell model (Mulloy et al., 2002; Wunderlich and Mulloy, 2009) of human CD34$^+$ progenitor cells transduced by A-E expressing lentivirus (Millington et al., 2009). Transfection of CD34$^+$/A-E cells with siRNA against RUNX1 (Figure S6) resulted in reduced expression of RUNX1 associated with an increased proportion of Annexin-V$^+$ positive cells as compared with cells transfected with control NT siRNA (Figure 7C and 7D). This finding indicates that RUNX1 activity is required for the preleukemic CD34$^+$/A-E cells viability and underscores the critical importance of the RUNX1/A-E balance for the leukemogenic process.

DISCUSSION

The evolvement of cancer cells involves the acquisition of several hallmark capabilities (Hanahan and Weinberg, 2000, 2011), including accelerated proliferation, self-renewal, and evasion of apoptosis. The prevailing notion is that t(8;21) AML is initiated by a chromosomal translocation that occurs in BM hematopoietic stem cells (HSCs). The resulting pre-LSCs that express the oncogenic fusion protein self-renew and persist in the BM (Goyama and Mulloy, 2011; Hatlen et al., 2012; Lam and Zhang, 2012). During AML development, these pre-LSCs undergo clonal transformation in a multistep process involving additional genetic alterations that abrogate cell-growth regulations (Thol and Ganser, 2010). The role of the chimeric A-E protein in the etiology of t(8;21) AML has been widely studied (Hatlen et al., 2012; Lam and Zhang, 2012). However, the importance of the native RUNX1 for the development of t(8;21) or inv(16) AML subtypes remained obscure (Goyama and Mulloy, 2011).

We have shown that expression of native RUNX1 is crucial for the survival of t(8;21) Kasumi-1 and inv(16) ME-1 AML cell lines, as evidenced by the fact that RUNX1 KD evoked apoptotic cell death. The medical significance of this leukemic cell addiction to native RUNX1 is underscored by clinical data (reviewed in Goyama and Mulloy, 2011) showing that active *RUNX1* is usually maintained in patients with t(8;21) and inv(16) AML, whereas the gene is frequently inactivated in other forms of AML (Döhner and Döhner, 2008; Heilman et al., 2006; Preudhomme et al., 2009;

Schnittger et al., 2011; Tang et al., 2009). Furthermore, WT RUNX1 is not only preserved but is frequently amplified in patients with t(12;21) B cell acute lymphoblastic leukemia (ALL) (Ma et al., 2001; Martínez-Ramírez et al., 2001; Peter et al., 2009), suggesting that WT RUNX1 is also instrumental in t(12;21) ALL development. However, a different mechanism underlies the requirement of *RUNX1* expression for cell growth of the t(4;11) mixed lineage leukemia (MLL) MV4-11 and SEM cell lines (Wilkinson et al., 2013).

Using *Z-VAD-FMK* and ImageStream System analysis, we demonstrated that RUNX1 KD-induced Kasumi-1 cell death is caspase dependent and associated with mitochondrial membrane depolarization. Significantly, this cell death involves A-E gain-of-function activity, as shown by the complete rescue from apoptosis upon A-E KD in Kasumi-1$^{RX1\text{-}KD}$ cells. Consistent with the involvement of A-E in Kasumi-1$^{RX1\text{-}KD}$ cell death, ChIP-seq and gene expression data demonstrated opposing effects of RUNX1 and A-E on their common target genes. Moreover, we showed that RUNX1 can indirectly modulate the expression of A-E uniquely regulated genes, suggesting that RUNX1 and A-E compete for common cooperating TFs. Upon RUNX1 KD, these TFs might be recruited by A-E, leading to the aberrant expression of RUNX1 uniquely regulated genes. This regulatory mechanism drives the overall alterations in gene expression that characterize Kasumi-1$^{RX1\text{-}KD}$ cells. Compatible with this interpretation, unique and shared A-E- and RUNX1-occupied regions are enriched for the motif of ETS TF family members that interact with the common DNA-binding domain of RUNX1 and A-E (Gu et al., 2000; Gunther and Graves, 1994; Kim et al., 1999).

The notion that A-E is involved in Kasumi-1$^{RX1\text{-}KD}$ cell death corresponds with the findings that A-E has inherent proapoptotic activity (Burel et al., 2001; Lu et al., 2006) that opposes its leukemogenicity. Our data suggest that WT RUNX1 counters this proapoptotic activity and thereby contributes to the long-term survival of t(8;21) preleukemic HSCs and consequently to the development of leukemia. Indeed, RUNX1 is highly expressed in CD34$^+$ long-term HSCs, where it transcriptionally regulates *CD34* expression (Levantini et al., 2011). Moreover, A-E-transduced CD34$^+$ hematopoietic cells yield highly proliferative cytokine-dependent cultures (Mulloy et al., 2002, 2003), suggesting that the proapoptotic activity of A-E in CD34$^+$ HSCs is attenuated. Similarly, ectopic expression of C-S in cultured CD34$^+$ hematopoietic cells produced long-term cell lines (Wunderlich et al., 2006). This finding is compatible with our observation that RUNX1 is also required for survival of the inv(16) leukemic cell line ME-1. It also supports the conclusion that the development of A-E- or C-S-mediated leukemia (CBF leukemias) (Speck and Gilliland, 2002) depends on a delicate balance between the oncogenic impact of the chimeric A-E and C-S proteins and the antiapoptotic activity of RUNX1. Accordingly, the two deletion mutants, A-E9a and CBFβ-SMMHC$_{d179\text{-}221}$, which accelerate leukemia development in mice, have a lower capacity to inhibit RUNX1 activity (Kamikubo et al., 2010; Kuo et al., 2006; Peterson et al., 2007; Yan et al., 2004, 2006, 2009), attesting to the crucial role of WT RUNX1 in the etiology of CBF leukemia. Collectively, these data indicate that RUNX1 effectively inhibits the chimeric protein-mediated apoptosis in leukemic cell lines, but at which step?

A large number of studies have reported that RUNX1 plays an important role in cell-cycle control by promoting G1 to S progression (reviewed in Friedman, 2009). We found that RUNX1 KD in the Kasumi-1 cell line caused enhanced A-E activity, resulting in decreased expression of key mitosis-regulatory genes. The aberrant expression of these RUNX1-regulated genes compromises mitotic functions, including SAC activity, leading to apoptosis. This finding uncovers a role of RUNX1 as a regulator of SAC functions and explains its importance for the viability of Kasumi-1 (and likely ME-1) leukemic cell lines. Of note, RUNX1 activity increases during G2/M due to Cdk-mediated phosphorylation of the protein (Friedman, 2009; Wang et al., 2007). During M phase, the SAC maintains genomic stability by delaying cell division until accurate chromosome segregation is achieved (Lara-Gonzalez et al., 2012). Defects in SAC function generate aneuploidy that could facilitate tumorigenesis (Holland and Cleveland, 2012; Kops et al., 2005). Therefore, it is possible that the initial reduction of RUNX1 activity in BM HSCs by t(8;21) translocation contributes to the accumulation of additional genetic alterations that are required for onset of leukemia (see Graphical Abstract). The finding that native RUNX1 is required for the viability of preleukemic CD34$^+$/A-E cells further supports this notion.

EXPERIMENTAL PROCEDURES

Cell Culture and Expression Analysis

Kasumi-1 cells were purchased from the ATCC and maintained in RPMI-1640 supplemented with 20% fetal bovine serum (FBS), 2 mM L-glutamine, and 1% penicillin-streptomycin at 37°C and 5% CO_2. ME-1 cells (Yanagisawa et al., 1991) were obtained from DSMZ and grown in RPMI-1640 medium with 20% heat-inactivated FBS. Further information regarding the western blot, qRT-PCR, and fluorescence-activated cell sorting (FACS) analyses is included in the Extended Experimental Procedures.

ChIP-Seq

Two biological replicate ChIP-seq experiments were done for the specific detection of either RUNX1- or AML1-ETO-bound genomic regions according to standard procedures previously summarized in (Pencovich et al., 2011), including several modifications as detailed in the Extended Experimental Procedures.

siRNA Transfection

RUNX1-targeting, A-E-targeting, or NT control siRNA oligos (Thermo Scientific Dharmacon) were electroporated into Kasumi-1, ME-1, and CD34$^+$ cells as detailed in the Extended Experimental Procedures.

Transcriptome Data Acquisition and Analysis

For transcriptome data acquisition, fluorescein isothiocyanate (FITC)-labeled NT siRNA oligos (#2013, Block-it fluorescent oligo; Life Technologies) were cotransfected with RUNX1-targeting, A-E-targeting, or control NT siRNAs, and FITC$^+$ cells were FACS isolated following 96 hr incubation. RNA was obtained using miRNeasy (QIAGEN), its integrity was assessed using Bioanalyzer (Agilent Technologies), and transcriptome analysis was conducted as previously described (Pencovich et al., 2011), including several modifications as detailed in the Extended Experimental Procedures.

Multispectral Imaging Flow Cytometry: ImageStream System Analysis

For multispectral imaging flow cytometry, approximately 10^4 siRNA-treated cells were collected per sample and data were analyzed using image analysis software (IDEAS 4.0; Amnis) as detailed in the Extended Experimental Procedures.

Generation of A-E-Expressing Human Hematopoietic Progenitor CD34$^+$ Cells

Human hematopoietic progenitor CD34$^+$ cells were purchased from Invitrogen (Life Technologies) and cultured according to the manufacturer's instructions. These StemPro CD34$^+$ cells are human cord blood hematopoietic progenitor cells derived from mixed donors. Human A-E cDNA was excised from Addgene (http://www.addgene.org) pUHD-A-E plasmid using Age I and subcloned into a modified Addgene pCSC lentiviral vector (Regev et al., 2010) downstream from the cytomegalovirus promoter and upstream from the internal ribosomal entry site (IRES)-GFP cassette. Recombinant pseudo-lentiviral particles were generated by cotransfection of the pCSC-A-E-IRES-GFP vector and packaging DNA plasmids into human embryonic kidney (HEK) 293T cells. Following isolation and purification of pCSC-A-E-IRES-GFP lentiviral particles, they were introduced into CD34$^+$ cells as previously described (Millington et al., 2009). Following lentiviral transduction, the cells were harvested and expression of A-E in HEK 293T and in GFP-expressing CD34$^+$ cells was validated by western blotting and qRT-PCR, respectively.

ACCESSION NUMBERS

The microarray and ChIP-seq data reported in this manuscript are available at the NCBI Gene Expression Omnibus under accession number GSE45748.

SUPPLEMENTAL INFORMATION

Supplemental Information includes Extended Experimental Procedures, five figures, and seven tables and can be found with this article online at http://dx.doi.org/10.1016/j.celrep.2013.08.020.

ACKNOWLEDGMENTS

We thank Dr. Daniela Amann-Zalcennstein and Dr. Shirely Horn-Saban for help with Illumina sequencing and gene expression data acquisition, Dr. Ziv Porat for ImageStream analysis, and Dr. Ditsa Levanon for helpful comments throughout this work. We thank Dr. Takashi Egawa for providing the anti-AP4 Ab, Prof. Alon Chen for the lentivirus vector, and Profs. Moshe Oren, Atan Gross, Eli Arama, Yaqub Hanna, Orly Reiner, Tsvee Lapidot, and Sigal Tavor for helpful suggestions and stimulating discussions. This study was supported by grants from the Israel Science Foundation and the European Research Council. A.T. is an incumbent of the Rich family WIS CDC.

Received: March 16, 2013
Revised: July 3, 2013
Accepted: August 8, 2013
Published: September 19, 2013

REFERENCES

Arthur, D.C., and Bloomfield, C.D. (1983). Association of partial deletion of the long arm of chromosome 16 and bone marrow eosinophilia in acute non-lymphocytic leukemia. Blood *62*, 931.

Asou, H., Tashiro, S., Hamamoto, K., Otsuji, A., Kita, K., and Kamada, N. (1991). Establishment of a human acute myeloid leukemia cell line (Kasumi-1) with 8;21 chromosome translocation. Blood *77*, 2031–2036.

Bakshi, R., Zaidi, S.K., Pande, S., Hassan, M.Q., Young, D.W., Montecino, M., Lian, J.B., van Wijnen, A.J., Stein, J.L., and Stein, G.S. (2008). The leukemogenic t(8;21) fusion protein AML1-ETO controls rRNA genes and associates with nucleolar-organizing regions at mitotic chromosomes. J. Cell Sci. *121*, 3981–3990.

Bee, T., Ashley, E.L., Bickley, S.R., Jarratt, A., Li, P.S., Sloane-Stanley, J., Göttgens, B., and de Bruijn, M.F. (2009). The mouse Runx1 +23 hematopoietic stem cell enhancer confers hematopoietic specificity to both Runx1 promoters. Blood *113*, 5121–5124.

Boyapati, A., Yan, M., Peterson, L.F., Biggs, J.R., Le Beau, M.M., and Zhang, D.E. (2007). A leukemia fusion protein attenuates the spindle checkpoint and promotes aneuploidy. Blood *109*, 3963–3971.

Burel, S.A., Harakawa, N., Zhou, L., Pabst, T., Tenen, D.G., and Zhang, D.E. (2001). Dichotomy of AML1-ETO functions: growth arrest versus block of differentiation. Mol. Cell. Biol. *21*, 5577–5590.

Cameron, E.R., and Neil, J.C. (2004). The Runx genes: lineage-specific oncogenes and tumor suppressors. Oncogene *23*, 4308–4314.

Castilla, L.H., Wijmenga, C., Wang, Q., Stacy, T., Speck, N.A., Eckhaus, M., Marín-Padilla, M., Collins, F.S., Wynshaw-Boris, A., and Liu, P.P. (1996). Failure of embryonic hematopoiesis and lethal hemorrhages in mouse embryos heterozygous for a knocked-in leukemia gene CBFB-MYH11. Cell *87*, 687–696.

Castilla, L.H., Perrat, P., Martinez, N.J., Landrette, S.F., Keys, R., Oikemus, S., Flanegan, J., Heilman, S., Garrett, L., Dutra, A., et al. (2004). Identification of genes that synergize with Cbfb-MYH11 in the pathogenesis of acute myeloid leukemia. Proc. Natl. Acad. Sci. USA *101*, 4924–4929.

Davis, J.N., McGhee, L., and Meyers, S. (2003). The ETO (MTG8) gene family. Gene *303*, 1–10.

de Bruijn, M.F., and Speck, N.A. (2004). Core-binding factors in hematopoiesis and immune function. Oncogene *23*, 4238–4248.

Döhner, K., and Döhner, H. (2008). Molecular characterization of acute myeloid leukemia. Haematologica *93*, 976–982.

Dunne, J., Cullmann, C., Ritter, M., Soria, N.M., Drescher, B., Debernardi, S., Skoulakis, S., Hartmann, O., Krause, M., Krauter, J., et al. (2006). siRNA-mediated AML1/MTG8 depletion affects differentiation and proliferation-associated gene expression in t(8;21)-positive cell lines and primary AML blasts. Oncogene *25*, 6067–6078.

Egawa, T., and Littman, D.R. (2011). Transcription factor AP4 modulates reversible and epigenetic silencing of the Cd4 gene. Proc. Natl. Acad. Sci. USA *108*, 14873–14878.

Erickson, P., Gao, J., Chang, K.S., Look, T., Whisenant, E., Raimondi, S., Lasher, R., Trujillo, J., Rowley, J., and Drabkin, H. (1992). Identification of breakpoints in t(8;21) acute myelogenous leukemia and isolation of a fusion transcript, AML1/ETO, with similarity to Drosophila segmentation gene, runt. Blood *80*, 1825–1831.

Friedman, A.D. (2009). Cell cycle and developmental control of hematopoiesis by Runx1. J. Cell. Physiol. *219*, 520–524.

Gardini, A., Cesaroni, M., Luzi, L., Okumura, A.J., Biggs, J.R., Minardi, S.P., Venturini, E., Zhang, D.E., Pelicci, P.G., and Alcalay, M. (2008). AML1/ETO oncoprotein is directed to AML1 binding regions and co-localizes with AML1 and HEB on its targets. PLoS Genet. *4*, e1000275.

Ghozi, M.C., Bernstein, Y., Negreanu, V., Levanon, D., and Groner, Y. (1996). Expression of the human acute myeloid leukemia gene AML1 is regulated by two promoter regions. Proc. Natl. Acad. Sci. USA *93*, 1935–1940.

Goyama, S., and Mulloy, J.C. (2011). Molecular pathogenesis of core binding factor leukemia: current knowledge and future prospects. Int. J. Hematol. *94*, 126–133.

Gu, T.L., Goetz, T.L., Graves, B.J., and Speck, N.A. (2000). Auto-inhibition and partner proteins, core-binding factor beta (CBFbeta) and Ets-1, modulate DNA binding by CBFalpha2 (AML1). Mol. Cell. Biol. *20*, 91–103.

Gunther, C.V., and Graves, B.J. (1994). Identification of ETS domain proteins in murine T lymphocytes that interact with the Moloney murine leukemia virus enhancer. Mol. Cell. Biol. *14*, 7569–7580.

Hanahan, D., and Weinberg, R.A. (2000). The hallmarks of cancer. Cell *100*, 57–70.

Hanahan, D., and Weinberg, R.A. (2011). Hallmarks of cancer: the next generation. Cell *144*, 646–674.

Hatlen, M.A., Wang, L., and Nimer, S.D. (2012). AML1-ETO driven acute leukemia: insights into pathogenesis and potential therapeutic approaches. Fr. Medecine *6*, 248–262.

Heidenreich, O., Krauter, J., Riehle, H., Hadwiger, P., John, M., Heil, G., Vornlocher, H.P., and Nordheim, A. (2003). AML1/MTG8 oncogene suppression by small interfering RNAs supports myeloid differentiation of t(8;21)-positive leukemic cells. Blood *101*, 3157–3163.

Heilman, S.A., Kuo, Y.H., Goudswaard, C.S., Valk, P.J., and Castilla, L.H. (2006). Cbfbeta reduces Cbfbeta-SMMHC-associated acute myeloid leukemia in mice. Cancer Res. *66*, 11214–11218.

Holland, A.J., and Cleveland, D.W. (2012). Losing balance: the origin and impact of aneuploidy in cancer. EMBO Rep. *13*, 501–514.

Hug, B.A., and Lazar, M.A. (2004). ETO interacting proteins. Oncogene *23*, 4270–4274.

Hyde, R.K., and Liu, P.P. (2010). RUNX1 repression-independent mechanisms of leukemogenesis by fusion genes CBFB-MYH11 and AML1-ETO (RUNX1-RUNX1T1). J. Cell. Biochem. *110*, 1039–1045.

Kamikubo, Y., Zhao, L., Wunderlich, M., Corpora, T., Hyde, R.K., Paul, T.A., Kundu, M., Garrett, L., Compton, S., Huang, G., et al. (2010). Accelerated leukemogenesis by truncated CBF beta-SMMHC defective in high-affinity binding with RUNX1. Cancer Cell *17*, 455–468.

Kim, W.Y., Sieweke, M., Ogawa, E., Wee, H.J., Englmeier, U., Graf, T., and Ito, Y. (1999). Mutual activation of Ets-1 and AML1 DNA binding by direct interaction of their autoinhibitory domains. EMBO J. *18*, 1609–1620.

Kops, G.J., Weaver, B.A., and Cleveland, D.W. (2005). On the road to cancer: aneuploidy and the mitotic checkpoint. Nat. Rev. Cancer *5*, 773–785.

Kuo, Y.H., Landrette, S.F., Heilman, S.A., Perrat, P.N., Garrett, L., Liu, P.P., Le Beau, M.M., Kogan, S.C., and Castilla, L.H. (2006). Cbf beta-SMMHC induces distinct abnormal myeloid progenitors able to develop acute myeloid leukemia. Cancer Cell *9*, 57–68.

Lam, K., and Zhang, D.E. (2012). RUNX1 and RUNX1-ETO: roles in hematopoiesis and leukemogenesis. Front Biosci (Landmark Ed) *17*, 1120–1139.

Lara-Gonzalez, P., Westhorpe, F.G., and Taylor, S.S. (2012). The spindle assembly checkpoint. Curr. Biol. *22*, R966–R980.

Le Beau, M.M., Larson, R.A., Bitter, M.A., Vardiman, J.W., Golomb, H.M., and Rowley, J.D. (1983). Association of an inversion of chromosome 16 with abnormal marrow eosinophils in acute myelomonocytic leukemia. A unique cytogenetic-clinicopathological association. N. Engl. J. Med. *309*, 630–636.

Levanon, D., Glusman, G., Bangsow, T., Ben-Asher, E., Male, D.A., Avidan, N., Bangsow, C., Hattori, M., Taylor, T.D., Taudien, S., et al. (2001). Architecture and anatomy of the genomic locus encoding the human leukemia-associated transcription factor RUNX1/AML1. Gene *262*, 23–33.

Levantini, E., Lee, S., Radomska, H.S., Hetherington, C.J., Alberich-Jorda, M., Amabile, G., Zhang, P., Gonzalez, D.A., Zhang, J., Basseres, D.S., et al. (2011). RUNX1 regulates the CD34 gene in haematopoietic stem cells by mediating interactions with a distal regulatory element. EMBO J. *30*, 4059–4070.

Licht, J.D. (2001). AML1 and the AML1-ETO fusion protein in the pathogenesis of t(8;21) AML. Oncogene *20*, 5660–5679.

Lu, Y., Xu, Y.B., Yuan, T.T., Song, M.G., Lübbert, M., Fliegauf, M., and Chen, G.Q. (2006). Inducible expression of AML1-ETO fusion protein endows leukemic cells with susceptibility to extrinsic and intrinsic apoptosis. Leukemia *20*, 987–993.

Lukasik, S.M., Zhang, L., Corpora, T., Tomanicek, S., Li, Y., Kundu, M., Hartman, K., Liu, P.P., Laue, T.M., Biltonen, R.L., et al. (2002). Altered affinity of CBF beta-SMMHC for Runx1 explains its role in leukemogenesis. Nat. Struct. Biol. *9*, 674–679.

Ma, S.K., Wan, T.S., Cheuk, A.T., Fung, L.F., Chan, G.C., Chan, S.Y., Ha, S.Y., and Chan, L.C. (2001). Characterization of additional genetic events in childhood acute lymphoblastic leukemia with TEL/AML1 gene fusion: a molecular cytogenetics study. Leukemia *15*, 1442–1447.

Martinez, N., Drescher, B., Riehle, H., Cullmann, C., Vornlocher, H.P., Ganser, A., Heil, G., Nordheim, A., Krauter, J., and Heidenreich, O. (2004). The oncogenic fusion protein RUNX1-CBFA2T1 supports proliferation and inhibits senescence in t(8;21)-positive leukaemic cells. BMC Cancer *4*, 44.

Martínez-Ramírez, A., Urioste, M., Contra, T., Cantalejo, A., Tavares, A., Portero, J.A., López-Ibor, B., Bernacer, M., Soto, C., Cigudosa, J.C., and Benítez, J. (2001). Fluorescence in situ hybridization study of TEL/AML1 fusion and other abnormalities involving TEL and AML1 genes. Correlation with cytogenetic findings and prognostic value in children with acute lymphocytic leukemia. Haematologica *86*, 1245–1253.

Martinez Soria, N., Tussiwand, R., Ziegler, P., Manz, M.G., and Heidenreich, O. (2009). Transient depletion of RUNX1/RUNX1T1 by RNA interference delays tumour formation in vivo. Leukemia *23*, 188–190.

Miller, J.D., Stacy, T., Liu, P.P., and Speck, N.A. (2001). Core-binding factor beta (CBFbeta), but not CBFbeta-smooth muscle myosin heavy chain, rescues definitive hematopoiesis in CBFbeta-deficient embryonic stem cells. Blood *97*, 2248–2256.

Miller, J., Horner, A., Stacy, T., Lowrey, C., Lian, J.B., Stein, G., Nuckolls, G.H., and Speck, N.A. (2002). The core-binding factor beta subunit is required for bone formation and hematopoietic maturation. Nat. Genet. *32*, 645–649.

Millington, M., Arndt, A., Boyd, M., Applegate, T., and Shen, S. (2009). Towards a clinically relevant lentiviral transduction protocol for primary human CD34 hematopoietic stem/progenitor cells. PLoS ONE *4*, e6461.

Miyoshi, H., Kozu, T., Shimizu, K., Enomoto, K., Maseki, N., Kaneko, Y., Kamada, N., and Ohki, M. (1993). The t(8;21) translocation in acute myeloid leukemia results in production of an AML1-MTG8 fusion transcript. EMBO J. *12*, 2715–2721.

Müller, A.M., Duque, J., Shizuru, J.A., and Lübbert, M. (2008). Complementing mutations in core binding factor leukemias: from mouse models to clinical applications. Oncogene *27*, 5759–5773.

Mulloy, J.C., Cammenga, J., MacKenzie, K.L., Berguido, F.J., Moore, M.A., and Nimer, S.D. (2002). The AML1-ETO fusion protein promotes the expansion of human hematopoietic stem cells. Blood *99*, 15–23.

Mulloy, J.C., Cammenga, J., Berguido, F.J., Wu, K., Zhou, P., Comenzo, R.L., Jhanwar, S., Moore, M.A., and Nimer, S.D. (2003). Maintaining the self-renewal and differentiation potential of human CD34+ hematopoietic cells using a single genetic element. Blood *102*, 4369–4376.

Okuda, T., Cai, Z., Yang, S., Lenny, N., Lyu, C.J., van Deursen, J.M., Harada, H., and Downing, J.R. (1998). Expression of a knocked-in AML1-ETO leukemia gene inhibits the establishment of normal definitive hematopoiesis and directly generates dysplastic hematopoietic progenitors. Blood *91*, 3134–3143.

Okumura, A.J., Peterson, L.F., Okumura, F., Boyapati, A., and Zhang, D.E. (2008). t(8;21)(q22;q22) Fusion proteins preferentially bind to duplicated AML1/RUNX1 DNA-binding sequences to differentially regulate gene expression. Blood *112*, 1392–1401.

Pencovich, N., Jaschek, R., Tanay, A., and Groner, Y. (2011). Dynamic combinatorial interactions of RUNX1 and cooperating partners regulates megakaryocytic differentiation in cell line models. Blood *117*, e1–e14.

Peter, A., Heiden, T., Taube, T., Körner, G., and Seeger, K. (2009). Interphase FISH on TEL/AML1 positive acute lymphoblastic leukemia relapses—analysis of clinical relevance of additional TEL and AML1 copy number changes. Eur. J. Haematol. *83*, 420–432.

Peterson, L.F., Boyapati, A., Ahn, E.Y., Biggs, J.R., Okumura, A.J., Lo, M.C., Yan, M., and Zhang, D.E. (2007). Acute myeloid leukemia with the 8q22;21q22 translocation: secondary mutational events and alternative t(8;21) transcripts. Blood *110*, 799–805.

Preudhomme, C., Renneville, A., Bourdon, V., Philippe, N., Roche-Lestienne, C., Boissel, N., Dhedin, N., André, J.M., Cornillet-Lefebvre, P., Baruchel, A., et al. (2009). High frequency of RUNX1 biallelic alteration in acute myeloid leukemia secondary to familial platelet disorder. Blood *113*, 5583–5587.

Ptasinska, A., Assi, S.A., Mannari, D., James, S.R., Williamson, D., Dunne, J., Hoogenkamp, M., Wu, M., Care, M., McNeill, H., et al. (2012). Depletion of RUNX1/ETO in t(8;21) AML cells leads to genome-wide changes in chromatin structure and transcription factor binding. Leukemia *26*, 1829–1841.

Regev, L., Ezrielev, E., Gershon, E., Gil, S., and Chen, A. (2010). Genetic approach for intracerebroventricular delivery. Proc. Natl. Acad. Sci. USA *107*, 4424–4429.

Rosenbauer, F., Koschmieder, S., Steidl, U., and Tenen, D.G. (2005). Effect of transcription-factor concentrations on leukemic stem cells. Blood *106*, 1519–1524.

Schnittger, S., Dicker, F., Kern, W., Wendland, N., Sundermann, J., Alpermann, T., Haferlach, C., and Haferlach, T. (2011). RUNX1 mutations are

frequent in de novo AML with noncomplex karyotype and confer an unfavorable prognosis. Blood *117*, 2348–2357.

Speck, N.A., and Gilliland, D.G. (2002). Core-binding factors in haematopoiesis and leukaemia. Nat. Rev. Cancer *2*, 502–513.

Tang, J.L., Hou, H.A., Chen, C.Y., Liu, C.Y., Chou, W.C., Tseng, M.H., Huang, C.F., Lee, F.Y., Liu, M.C., Yao, M., et al. (2009). AML1/RUNX1 mutations in 470 adult patients with de novo acute myeloid leukemia: prognostic implication and interaction with other gene alterations. Blood *114*, 5352–5361.

Thol, F., and Ganser, A. (2010). Molecular pathogenesis of acute myeloid leukemia: a diverse disease with new perspectives. Front. Med. China *4*, 356–362.

Wang, Q., Stacy, T., Binder, M., Marin-Padilla, M., Sharpe, A.H., and Speck, N.A. (1996). Disruption of the Cbfa2 gene causes necrosis and hemorrhaging in the central nervous system and blocks definitive hematopoiesis. Proc. Natl. Acad. Sci. USA *93*, 3444–3449.

Wang, S., Zhang, Y., Soosairajah, J., and Kraft, A.S. (2007). Regulation of RUNX1/AML1 during the G2/M transition. Leuk. Res. *31*, 839–851.

Wilkinson, A.C., Ballabio, E., Geng, H., North, P., Tapia, M., Kerry, J., Biswas, D., Roeder, R.G., Allis, C.D., Melnick, A., et al. (2013). RUNX1 is a key target in t(4;11) leukemias that contributes to gene activation through an AF4-MLL complex interaction. Cell Rep *3*, 116–127.

Wunderlich, M., and Mulloy, J.C. (2009). Model systems for examining effects of leukemia-associated oncogenes in primary human CD34+ cells via retroviral transduction. Methods Mol. Biol. *538*, 263–285.

Wunderlich, M., Krejci, O., Wei, J., and Mulloy, J.C. (2006). Human CD34+ cells expressing the inv(16) fusion protein exhibit a myelomonocytic phenotype with greatly enhanced proliferative ability. Blood *108*, 1690–1697.

Yan, M., Burel, S.A., Peterson, L.F., Kanbe, E., Iwasaki, H., Boyapati, A., Hines, R., Akashi, K., and Zhang, D.E. (2004). Deletion of an AML1-ETO C-terminal NcoR/SMRT-interacting region strongly induces leukemia development. Proc. Natl. Acad. Sci. USA *101*, 17186–17191.

Yan, M., Kanbe, E., Peterson, L.F., Boyapati, A., Miao, Y., Wang, Y., Chen, I.M., Chen, Z., Rowley, J.D., Willman, C.L., and Zhang, D.E. (2006). A previously unidentified alternatively spliced isoform of t(8;21) transcript promotes leukemogenesis. Nat. Med. *12*, 945–949.

Yan, M., Ahn, E.Y., Hiebert, S.W., and Zhang, D.E. (2009). RUNX1/AML1 DNA-binding domain and ETO/MTG8 NHR2-dimerization domain are critical to AML1-ETO9a leukemogenesis. Blood *113*, 883–886.

Yanagisawa, K., Horiuchi, T., and Fujita, S. (1991). Establishment and characterization of a new human leukemia cell line derived from M4E0. Blood *78*, 451–457.

Yergeau, D.A., Hetherington, C.J., Wang, Q., Zhang, P., Sharpe, A.H., Binder, M., Marín-Padilla, M., Tenen, D.G., Speck, N.A., and Zhang, D.E. (1997). Embryonic lethality and impairment of haematopoiesis in mice heterozygous for an AML1-ETO fusion gene. Nat. Genet. *15*, 303–306.

Zhang, J., Kalkum, M., Yamamura, S., Chait, B.T., and Roeder, R.G. (2004). E protein silencing by the leukemogenic AML1-ETO fusion protein. Science *305*, 1286–1289.